Received by *Research Archive*: 2026-07-01
Peer-reviewed version: *Journal of Scientific and Mathematical Research* **6** (2026) pp. 95-108
jscimath/pubs/J202606-095TM.pdf

Comparison of operational efficiency of electric and gasoline transportation systems

Thad S. Morton

A comparison of the operational energy efficiency of representative gasoline-powered and battery-electric vehicle transportation systems is presented. Rather than comparing only engine or motor efficiencies, the analysis follows the principal operational energy conversions leading to mechanical work at the vehicle. A representative gasoline-powered transportation system is found to have a higher overall operational energy efficiency than the battery-electric alternative.

1. Introduction

The purpose of this work is to provide a back-to-back comparison of internal-combustion-engine and battery-electric-vehicle (BEV) transportation systems. BEV efficiencies of 77% to 95% are commonly reported in the literature (Sweeting *et al.* 2011; Faria *et al.* 2012; Liu *et al.* 2021; Loy-Benitez *et al.* 2021; McKenzie 2021; Pokharel *et al.* 2021; Sheng *et al.* 2021; Sandoval 2023; Dababneh *et al.* 2025; Waseem *et al.* 2025). When interpreted as operational efficiencies of the transportation system, however, these values implicitly assign efficiencies of 100% to both electricity generation and grid delivery. The frequency with which such interpretations are made indicates that this unequal-boundary comparison is widespread rather than exceptional. The reported efficiency comparisons do not represent equivalent portions of the two energy pathways. The high reported BEV efficiencies begin with electricity already generated. In this work, the performance of a commercially produced gasoline engine is reconstructed from its operating specifications and thermodynamic cycle, and its fuel-to-work efficiency is compared with that of existing-grid electric transportation.

2. The Gasoline Engine Efficiency

As a concrete example, consider the Buick 3.8-liter 3800 Series III V6 engine (naturally aspirated) that was used in the Pontiac Grand Prix, 2004–2008, the Buick LaCrosse, 2005–2009, and the Buick Lucerne, 2006–2008. It produces 200 hp (149 kW) of power at 5200 rpm, with compression ratio of 9.4, bore of 3.8 in, and stroke of 3.4 in. This engine is selected not because it is the most efficient gasoline engine available, but because it is representative of technology whose performance is already widely demonstrated in commercial service.

Since we know the power produced by the engine, we can find the peak temperature seen in the cylinders and hence the rate at which heat is lost through the engine block.

3800 Series III
2005 3.8L V-6 (L26)

The thermodynamic state of the gas in the engine cylinder during one cycle is described by the cycle diagram shown in Figure 1. The net specific work output from the engine during one cycle is given by the following integral:

$$w_{\text{cycle}} \;=\; \oint p\,\mathrm{d}v \tag{1}$$

Here, p and v are the pressure and specific volume of the gas inside the cylinders. Expanding (1) for this 4-stroke engine, we have

$$w_{\text{cycle}} \;=\; \int_1^2 p\,\mathrm{d}v \;+\; \int_2^3 \cancel{p\,\mathrm{d}v} \;+\; \int_3^4 p\,\mathrm{d}v \;+\; \int_4^1 \cancel{p\,\mathrm{d}v}\,. \tag{2}$$

In the spark-ignition engine (the Otto cycle), work is put into the working fluid during the compression stroke from State 1 to State 2, and work is extracted from the working fluid during the expansion stroke, or power stroke, from State 3 to State 4. When the piston is at top-dead center, no work is done because there is momentarily no displacement of the piston. It is here, at top dead center (or just before it), that heat is added by combustion initiated by the spark (process 2-3 in Figure 1). Between States 4 and 1 the valve is opened during the exhaust and intake strokes, so the cylinder pressure is nearly atmospheric throughout.

Start with the fact that the compression ratio r is the ratio of $\cancel{V}_1$, the piston volume at intake, to $\cancel{V}_2$, the piston volume after compression:

$$r = \frac{\cancel{V}_1}{\cancel{V}_2} = \frac{v_1}{v_2} \qquad \text{and} \qquad \cancel{V}_1 = \cancel{V}_4, \quad \cancel{V}_2 = \cancel{V}_3, \quad v_1 = v_4, \quad v_2 = v_3$$

Also, the specific volume v_1 at State 1 is, by the ideal gas law,

$$v_1 \;=\; \frac{RT_1}{P_1} \;=\; \frac{287\ \text{kJ}}{\text{kg}}\bigg|\frac{300\ \text{K}}{100\ \text{kPa}} \;=\; 0.861\,\text{m}^3/\text{kg}\,.$$

This allows us to compute all specific volumes. With these values, we begin to construct a table of thermodynamic properties such as Table 1.

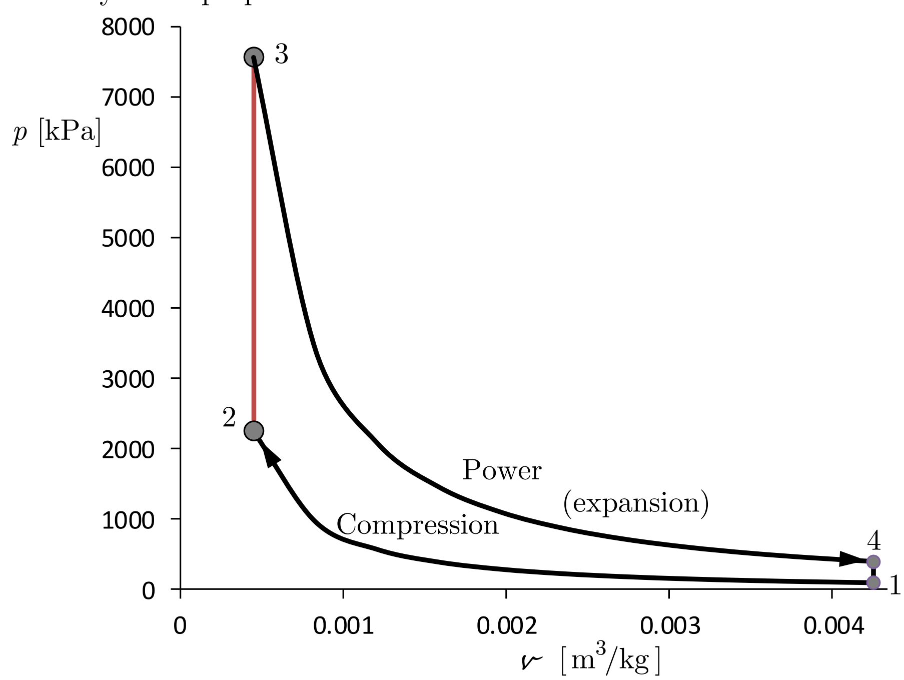

Figure 1. A closed line integral of pressure and specific volume yields the net work of the engine per cycle.

State	T [K]	P [kPa]	u [kJ/kg]	v [m^3/kg]	k
1	300	100		0.861	1.39
2				0.0916	
3				0.0916	1.3
4				0.861	

Table 1. Table of thermodynamic properties in engine.

With a known displacement volume $\mathcal{V}_D$ of 3.8 liters, the total volume $\mathcal{V}_1$ at State 1, which includes the clearance volume $\mathcal{V}_C = \mathcal{V}_2$ can be found using the compression ratio r:

$$r \;=\; \frac{\mathcal{V}_1}{\mathcal{V}_2} \;=\; \frac{(\mathcal{V}_C + \mathcal{V}_D)}{\mathcal{V}_C} \qquad \rightarrow \qquad \mathcal{V}_C \;=\; \frac{\mathcal{V}_D}{(r-1)}\,. \tag{3}$$

Therefore, $\mathcal{V}_1$ is

$$\mathcal{V}_1 \;=\; (\mathcal{V}_C + \mathcal{V}_D) \;=\; r\,\mathcal{V}_D/(r-1) \;=\; 0.00425 \text{ m}^3\,,$$

and the total mass of air in the engine is

$$m_{\text{Tot}} = \mathcal{V}_1/v_1 = 0.004939 \text{ kg}\,. \tag{4}$$

The two work processes on the right side of (2) are nearly isentropic, so p_2 and T_2 are given by the isentropic relations:

$$p_2 = p_1\left(\frac{v_1}{v_2}\right)^{\gamma} = p_1\, r^{\gamma} \qquad \text{and} \qquad T_2 \;=\; T_1\left(\frac{v_1}{v_2}\right)^{\gamma-1} \;=\; T_1\, r^{\gamma-1}\,,$$

where γ is the ratio of specific heats c_p/c_v of the gas, which is around $\gamma = 1.39$ between these temperatures, and r is the compression ratio of the engine, known to be $r = 9.4$. So with an intake temperature of 300 K, the pressure and temperature after the compression process are

$$p_2 = p_1\, r^{\gamma} = 100\,\text{kPa}\,(9.4)^{1.39} \qquad\qquad T_2 = T_1\, r^{\gamma-1}$$

$$= 2252.4\,\text{kPa} \qquad\qquad = 718.9\,\text{K}$$

During process 1-2, the pressure function is given by

$$p = p_1\left(\frac{v_1}{v}\right)^{\gamma},$$

and during the power stroke from state 3 to state 4, it is

$$p = p_3\left(\frac{v_3}{v}\right)^{\gamma}.$$

These functions can be substituted into the two integrals in (2), giving

$$w_{\text{cycle}} \;=\; \int_1^2 p_1\left(\frac{v_1}{v}\right)^{\gamma} \mathrm{d}v \;+\; \int_3^4 p_3\left(\frac{v_3}{v}\right)^{\gamma} \mathrm{d}v\,,$$

For accuracy purposes, the ratios of specific heats γ are taken from data midway between states as suggested in Table 1. For example, between states 1 and 2, the following notation will be used henceforth γ_{12}, instead of γ. The above relation integrates to

$$w_{\text{cycle}} = \underbrace{\frac{p_1 v_1}{1-\gamma_{12}}\; r^{\gamma_{12}-1} - 1}_{\text{compression stroke}} + \underbrace{\frac{p_3 v_3}{1-\gamma_{34}}\left[r^{1-\gamma_{34}} - 1\right]}_{\text{power stroke}}. \tag{5}$$

Solving for the pressure p_3 gives

$$p_3 = \left[w_{\text{cycle}} - \frac{p_1 v_1}{1-\gamma_{12}}\left(r^{\gamma_{12}-1} - 1\right)\right]\frac{1-\gamma_{34}}{v_3\left(r^{1-\gamma_{34}} - 1\right)} \tag{6}$$

Then compute the net specific work done per cycle:

$$w_{\text{cycle}} = \frac{\dot{W}_{\text{net}}}{\dot{m}}, \tag{7}$$

where $\dot{W}_{\text{net}}$ is the net power, and by (4), the mass flow rate $\dot{m}$ is

$$\begin{aligned} \dot{m} &= m_{\text{Tot}}\,\Omega \\ &= \frac{0.00494 \text{ kg}}{\text{cycle}}\left|\frac{5200 \text{ rev}}{\text{min}}\right|\frac{1 \text{ min}}{60\text{s}}\left|\frac{1 \text{ cycle}}{2 \text{ rev}}\right. \\ \dot{m} &= 0.214 \text{ kg/s}. \end{aligned} \tag{8}$$

Here, Ω denotes the rotation rate of the shaft. (This is a 4-stroke engine, and two strokes of the piston make one revolution, so there are 2 revolutions per cycle.) Then (7) gives the net specific work done per cycle:

$$\begin{aligned} w_{\text{cycle}} &= 200 \text{ hp}\frac{0.7454 \text{ kJ}}{1 \text{ hp} \;\; \text{s}}\left|\frac{\text{s}}{0.214 \text{ kg}}\right. \\ &= 697 \text{ kJ/kg}. \end{aligned}$$

Now that w_{cycle} is known, the peak pressure at the beginning of the power stroke can be found from (6) to be $p_3 = 6{,}724$ kPa. Then the ideal gas law requires that

$$T_3 = p_3 T_2 / p_2 = 2146 \text{ K}.$$

The process from State 3 to 4 is isentropic, so State 4 is given by

$$p_4 = p_3\left(\frac{1}{r}\right)^{\gamma_{34}} = 365 \text{ kPa} \qquad \text{and} \qquad T_4 = T_3\left(\frac{1}{r}\right)^{\gamma_{34}-1} = 1096 \text{ K},$$

The updated table of thermodynamic properties is now as shown in Table 2. The internal energies u_2, u_3, and u_4 were interpolated from thermodynamic property data.

State	T [K]	P [kPa]	u [kJ/kg]	v [m^3/kg]	k
1	300	100	214	0.861	1.39
2	719	2,252	528	0.0916	
3	2,146	6,724	1820	0.0916	1.3
4	1096	365	841	0.861	

Table 2. Table of thermodynamic properties in engine.

We can find the specific work of the compression stroke and the power stroke separately by substituting the necessary thermodynamic properties back into (5):

$$w_{\text{cycle}} = \underbrace{-308.2\,\tfrac{\text{kJ}}{\text{kg}}}_{\substack{\text{compression}\\ \text{stroke}}} + \underbrace{1004.8\,\tfrac{\text{kJ}}{\text{kg}}}_{\substack{\text{power}\\ \text{stroke}}} = 697\,\tfrac{\text{kJ}}{\text{kg}}$$

We can convert these values to kilowatts by again multiplying by $\dot{m}$ given in (8). The power consumed by compression in the engine is therefore

$$\begin{aligned}\dot{W}_{\text{compr}} &= \dot{m}\,w_{\text{compr}} = \frac{0.214\text{ kg}}{\text{s}}\left|\frac{308.2\text{ kJ}}{\text{kg}}\right. \\ &= 66\text{ kW},\end{aligned}$$

and the power generated by the power stroke is

$$\begin{aligned}\dot{W}_{\text{expansion}} &= \dot{m}\,w_{\text{expansion}} = \frac{0.214\text{ kg}}{\text{s}}\left|\frac{1004.8\text{ kJ}}{\text{kg}}\right. \\ &= 215\text{ kW}.\end{aligned}$$

So the net work output is

$$\dot{W}_{\text{net}} = (\dot{W}_{\text{expansion}} - \dot{W}_{\text{compr}}) = (215\text{ kW} - 66\text{ kW}) = 149\text{ kW}\,. \tag{9}$$

State 3 is attained by adding heat from the fuel to State 2, so the heat added per cycle is:

$$\begin{aligned}q_{\text{in}} &= u_3 - u_2 \\ &= 1{,}292\text{ kJ/kg}\end{aligned}$$

Converting to kilowatts again using (8) gives:

$$\begin{aligned}\dot{Q}_{\text{in}} &= \dot{m}\,q_{\text{in}} = \frac{0.214\text{ kg}}{\text{s}}\left|\frac{1{,}292\text{ kJ}}{\text{kg}}\right| \\ &= 277\text{ kW}\end{aligned} \tag{10}$$

Therefore, the thermal efficiency is

$$\eta_{\text{th}} = \frac{\dot{W}_{\text{net}}}{\dot{Q}_{\text{in}}} = \frac{149\text{ kW}}{277\text{ kW}} = 54\%\,.$$

Energy is rejected to the exhaust at a rate of

$$\begin{aligned}\dot{Q}_{\text{out}} &= \dot{m}(u_4 - u_1) = 0.214\,\frac{\text{kg}}{\text{s}}(841 - 214)\frac{\text{kJ}}{\text{kg}} \\ &= 134\text{ kW}\end{aligned}$$

We can compare the rate at which energy is supplied to the working fluid in (10) with the energy supplied by the fuel, as given by the heating value of gasoline, $h_{\text{fuel}} = 44{,}000\,\text{kJ/kg}$. For a stoichiometric air-fuel ratio (which, for gasoline, is $AFR = 14.6$), the amount of fuel used per cycle is

$$m_{\text{fuel}} = \Delta m_{\text{air}}\frac{m_{\text{fuel}}}{m_{\text{air}}} = \frac{\Delta m_{\text{air}}}{AFR}\,, \tag{11}$$

where Δm_{air} is the mass of air brought into the engine by displacement of the piston, namely $\Delta m_{\text{air}} = \mathcal{V}_D\,/\,v_1$, which can be found from (3) to be

$$\Delta m_{\text{air}} = \mathcal{V}_C (r-1) \,/\, v_1 = 0.004413 \text{ kg}\,.$$

Then the mass of fuel per cycle is found from (11) to be $m_{\text{fuel}} = 0.283\,\text{g/cycle}$. So the heat added between states 2 and 3 is

$$\begin{aligned}\dot{Q}_{\text{fuel}} &= m_{\text{fuel}}\, h_{\text{fuel}}\, \Omega = \frac{0.283\text{ g}}{\text{cycle}}\left|\frac{44{,}000\text{ kJ}}{\text{kg}}\right|\frac{5200\text{ rev}}{\text{min}}\left|\frac{1\,\text{min}}{60s}\right|\frac{1\text{ cycle}}{2\text{ rev}} \\ &= 540\text{ kW}\end{aligned}$$

Fuel supplies energy at this rate, so the overall efficiency of this gasoline engine is, from (9),

$$\boxed{\eta = \frac{\dot{W}_{\text{net}}}{\dot{Q}_{\text{fuel}}} \approx \frac{149\text{ kW}}{540\text{ kW}} \approx 28\%} \tag{12}$$

According to (10), only 277 kW (not 540 kW) goes into the working fluid. This means that energy is being lost somewhere at a rate of

$$\begin{aligned}\dot{Q}_{\text{Lost}} &= \dot{Q}_{\text{Fuel}} - \dot{Q}_{\text{in}} = 540\text{ kW} - 277\text{ kW} \\ &= 263\text{ kW}\end{aligned}$$

But the exhausted energy has already been accounted for in $\dot{Q}_{\text{out}}$, so where does $\dot{Q}_{\text{Lost}}$ go if not out the exhaust? The quantity $\dot{Q}_{\text{Lost}}$ is the rate at which heat is taken from the engine block predominantly by the coolant or by air convection. Most of it is carried away by the coolant circulating through the engine block. It is a consequence of temperature limitations imposed by the engine materials.

By calculating the ratio

$$\frac{\dot{Q}_{\text{Lost}}}{\dot{Q}_{\text{out}}} = \frac{263\text{ kW}}{134\text{ kW}} = 1.96\,,$$

we find that nearly twice as much energy is extracted from the engine block as is sent to the exhaust pipe. It is this nearly inexhaustible supply of "waste" heat that allows the internal combustion engine efficiency to pull even farther ahead of the electric vehicle during winter driving. When the driver needs heat, "waste" heat is the best type of energy because it is free and is low-quality energy. In contrast, the electric vehicle must use high-quality (highly organized) electric energy and convert it to low-quality energy in order to heat the passengers. This process is characterized by high entropy generation.

As an independent check, the fuel consumption used in calculating the efficiency in (12) corresponds to a brake-specific fuel consumption of approximately 296 g/kWh (0.49 lb/hp·h). This value is consistent with the high-speed, high-load region of the generic 3.3-L naturally aspirated V6 gasoline-engine BSFC map reported by Dick *et al.* (2013) and reproduced by the National Research Council (2015).

3. Efficiency of the Electric Vehicle Option

3.1 System Overview

The power supply system for the electric vehicle is shown in Figure 2. With the exception of solar photovoltaics and reciprocating engines, which together constitute less than 6% of grid power generation, a working fluid spins a turbine that turns a generator. Electricity from the generator is transformed to high voltage/low current power so that it can be transmitted economically along power lines, after which its voltage is stepped down to the usable 240V/120V level for home use. The process will be examined next.

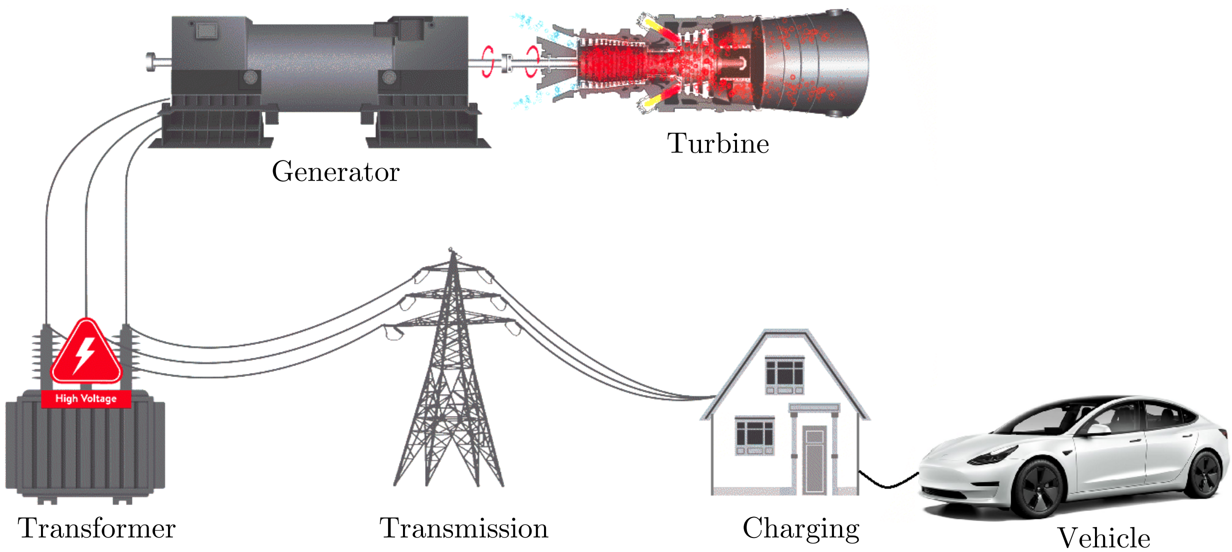

Figure 2. Energy generation and delivery system for the electric vehicle. (Composite illustration assembled from stock images: GE F-class gas turbine/generator; Tesla)

3.2 Power Plant

Consider the GE 7FA gas turbine burning natural gas. It usually operates at a firing temperature of about 2420°F (1600 K) with a pressure ratio of 16.13 (GE Energy 2009). From this information we can determine the thermal efficiency. The given information is shown in Table 3.

State	T [K]	p [kPa]	h [kJ/kg]	k
1	300	100		
2		1613		
3	1600	1613		
4		100		

Table 3. Gas properties at states in a typical gas turbine cycle.

The cycle is shown in Figure 3 in terms of temperature T and entropy s. The work process in the compressor is approximately isentropic, so the temperature T_2 at the compressor exit can be computed from the isentropic relations:

$$T_2 = T_1\left(\frac{p_1}{p_2}\right)^{\frac{\gamma-1}{\gamma}} = 300\left(\frac{1613}{100}\right)^{\frac{1.39-1}{1.39}}$$

$$= 654.6 \text{ K}$$

The process of work extraction from the turbine is also approximately isentropic, so the isentropic relation also gives the temperature T_4 at the turbine exhaust:

$$T_4 = T_3\left(\frac{p_4}{p_3}\right)^{\frac{\gamma-1}{\gamma}} = T_3\left(\frac{p_3}{p_4}\right)^{\frac{-(\gamma-1)}{\gamma}} = 1600(16.13)^{(1-1.32)/1.32} = 815.4 \text{ K}$$

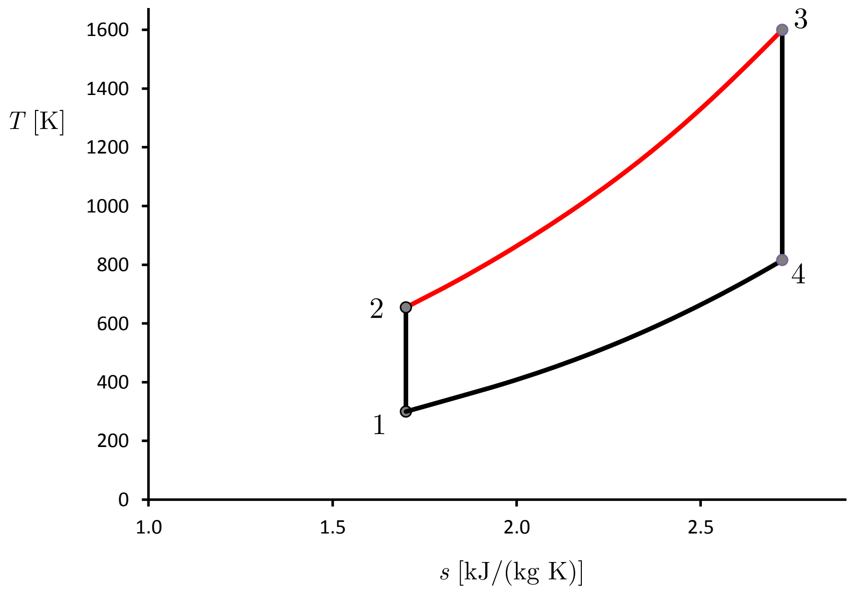

Figure 3. T-s diagram of gas turbine (Brayton) cycle.

The enthalpy h at each state is then taken from known gas property tables. The results are listed in Table 4.

The thermal efficiency is then given by

$$\eta_{\text{th}} = \frac{w_{\text{net}}}{q_{\text{in}}} = \frac{w_{\text{out}} - w_{\text{in}}}{q_{\text{in}}} = \frac{(h_4 - h_3) - (h_2 - h_1)}{h_3 - h_2}$$

Substituting values gives:

$$\eta_{\text{th}} = 0.506 .$$

State	T [K]	p [kPa]	h [kJ/kg]	k
1	300	100	300.01	1.39
2	654.6	1613	665.07	
3	1600	1613	1757.53	1.32
4	815.4	100	839.35	

Table 4. Gas properties at states in a typical gas turbine cycle.

The above value $\eta_{\text{th}} = 0.506$ is the thermal efficiency of the turbine/compressor/combustor combination if all components are perfectly efficient. However, the efficiency of the turbine above is around $\eta_{\text{turb}} = 94\%$ due to endwall losses and rotor and stator cooling flows that are taken from the mid-stages of the compressor in order to cool hot spots in the turbine. The compressor blades see similar losses though less pronounced than those of the turbine because cooling is not required and because the redirecting of the flow (blade turning) in the compressor is less aggressive due to its adverse (increasing) pressure gradient, unlike that of the turbine blades which operate in a favorable pressure gradient and so are very unlikely to stall. Because of the less aggressive turning, the compressor has many more blade rows than the turbine, each with its own losses. Consequently, the compressor efficiency is typically around $\eta_{\text{compr}} = 87.7\%$. These component efficiencies further reduce the efficiency from η_{th} to η'_{th}. These will be computed next.

The work of the compressor and turbine are

$$w_{c,s} = c_p(T_{2s} - T_1) \qquad \text{and} \qquad w_{t,s} = c_p(T_3 - T_{4s}) \tag{13}$$

Here, the subscript "s" denotes the isentropic (without the efficiency effect) quantities. For example, $w_c = w_{c,s}/\eta_c$ and $w_t = \eta_t\, w_{t,s}$ (the compressor must do more work, and the turbine does less work).

The ideal heat addition by the fuel is

$$q_{\text{in},s} = c_p(T_3 - T_{2s}), \tag{14}$$

but the actual compressor exit temperature is higher, so the actual heat addition is slightly less $[(q_{\text{in}} = q_{\text{in},s} - w_{c,s}(1/\eta_c - 1)]$. Then the efficiency of the turbine/compressor system is

$$\eta'_{\text{th}} = \frac{\eta_t\, w_{t,s} - w_{c,s}/\eta_c}{q_{\text{in},s} - w_{c,s}(1/\eta_c - 1)}. \tag{15}$$

Using constant specific heats, we can substitute (13) and (14) into this relation and obtain

$$\eta'_{\text{th}} = \frac{\eta_t(T_3 - T_{4s}) - (T_{2s} - T_1)/\eta_c}{(T_3 - T_{2s}) - (T_{2s} - T_1)(1/\eta_c - 1)}.$$

Substituting temperatures from Table 4 gives the actual thermal efficiency of turbine/compressor unit:

$$\eta'_{\text{th}} = 0.372.$$

The combustor efficiency is about $\eta_{\text{comb}} = 99\%$, and the generator efficiency is approximately $\eta_{\text{gen}} = 0.99$, so the power plant efficiency becomes:

$$\begin{aligned}\eta_{\text{plant}} &= \eta_{\text{gen}}\,\eta_{\text{comb}}\,\eta'_{\text{th}} \\ &= (0.99)(0.99)(0.372) \\ &= 0.365 \qquad\qquad \text{(7FA gas turbine)}\end{aligned} \tag{16}$$

This is close to the measured value $\eta_{\text{plant}} = 0.369$ reported by GE Energy (2009) for this 7FA gas turbine operating with a firing temperature of 2420°F. (The measured efficiency $\eta_{\text{th}}{}'$ can be computed from GE's reported "heat rate" by non-dimensionalizing its reciprocal.) As will be seen in Figure 4, this is higher than the average of the installed base of simple cycle (S.C.) gas turbine power plants, which is about 31%.

The example explained above is only one of a host of power generation options. Natural gas is presently the largest source of U.S. electricity generation. Its simple-cycle efficiency ranges from 32% to 41%; however, since gas turbines have higher exhaust temperatures than steam power plants, during approximately the last 30 years, gas turbine exhaust gas has increasingly been used as supply heat for a steam turbine "bottoming cycle." These combined-cycle (C.C.) systems are more efficient; the average tested heat rate reported by the U.S. Energy Information Administration for natural-gas combined-cycle units in 2024 corresponds to an efficiency of approximately 45.2% (USEIA 2025b). Efficiencies can be obtained by computing the dimensionless reciprocal of published heat rates. Figure 4 shows a pie chart of the different energy sources of the U.S. electric grid, along with a table of representative conversion efficiencies for each source. Technology-specific natural-gas efficiencies are based on EIA average tested heat rates, while operating heat rates are used where technology-specific operating heat rates are unavailable.

The energy generated by a specific type of power plant can be written using the national share f_i of that type of power, as follows: $E_{\text{out},i} = f_i E_{\text{out}}$. Therefore,

$$E_{\text{out},i} = f_i E_{\text{out}}, \tag{17}$$

where

$$\sum_i E_{\text{out},i} = \sum_i f_i E_{\text{out}} = E_{\text{out}} \tag{18}$$

since $\sum f_i = 1$. The efficiency η_i relates the energy generated $E_{\text{out},i}$ to the energy supplied $E_{\text{in},i}$, as follows: $E_{\text{out},i} = \eta_i E_{\text{in},i}$. So that

$$E_{\text{in},i} = \frac{E_{\text{out},i}}{\eta_i}. \tag{19}$$

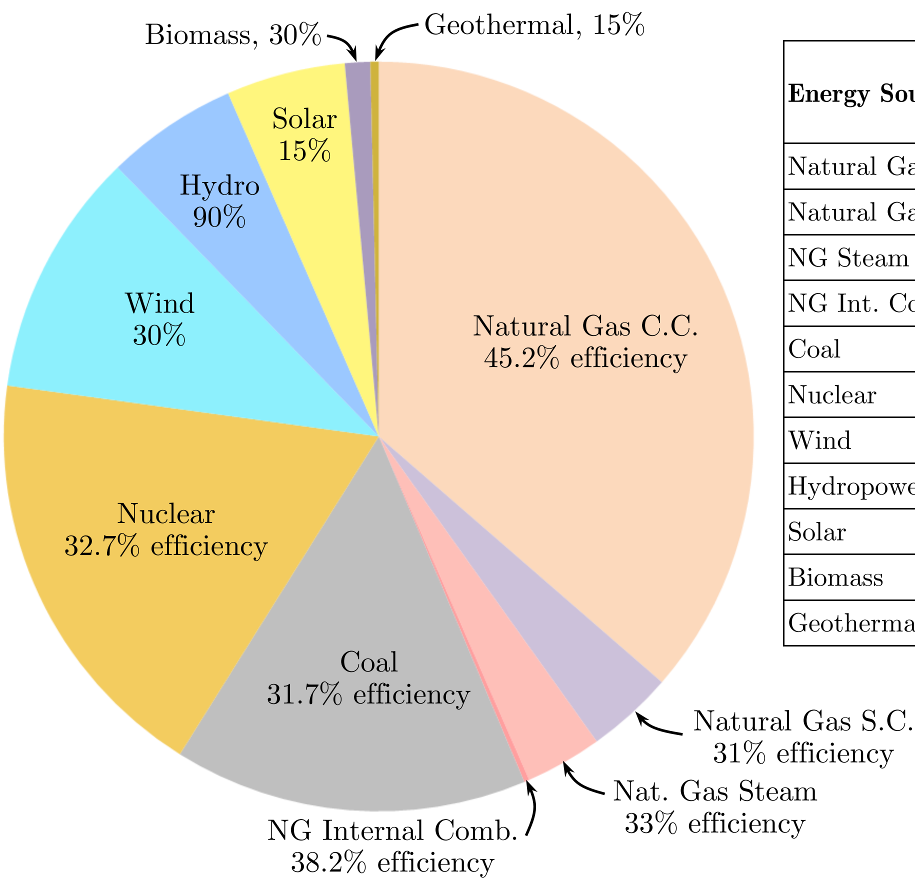

Energy Source	**Gen. Share** f_i	**Efficiency** η_i
Natural Gas C.C.	0.361	0.452
Natural Gas S.C.	0.037	0.310
NG Steam	0.033	0.330
NG Int. Comb.	0.002	0.382
Coal	0.151	0.317
Nuclear	0.182	0.327
Wind	0.105	0.30
Hydropower	0.056	0.90
Solar	0.051	0.15
Biomass	0.011	0.30
Geothermal	0.004	0.15

Figure 4. 2024 U.S. utility-scale net electricity generation shares and average efficiencies. Generation: USEIA (2025c,d); fossil-fuel and nuclear efficiencies: USEIA (2025a,b); renewable efficiencies: Evans *et al.* (2009).

We can write the total energy supplied as

$$E_{\text{in}} = \sum_i E_{\text{in},i} \tag{20}$$

Substituting (19) into the right side of (20) gives

$$E_{\text{in}} = \sum_i \frac{E_{\text{out},i}}{\eta_i}$$

and substituting (17) into the right side gives

$$E_{\text{in}} = \sum_i \frac{f_i\, E_{\text{out}}}{\eta_i}.$$

Solving for $E_{\text{out}}/E_{\text{in}}$ gives the aggregate efficiency of the national grid:

$$\eta_{\text{plant}} = \frac{E_{\text{out}}}{E_{\text{in}}} = \frac{1}{\sum_i (f_i/\eta_i)}.$$

Since some minor categories are not included, $\sum f_i = 0.9931$ rather than 1; therefore, the above relation should be more accurately written as:

$$\eta_{\text{plant}} = \frac{\sum f_i}{\sum_i (f_i/\eta_i)}. \tag{21}$$

Using values of f_i and η_i given in the table in Figure 4, the average generation-weighted efficiency of U.S. power plants is computed to be

$$\eta_{\text{plant}} \approx 0.347 \qquad \text{(average U.S. power plant)} \tag{22}$$

3.3 Transmission & Distribution Efficiency

The efficiency for conveying electricity from the plant to the location of use is determined by the following: a step-up transformer efficiency from the generator to the transmission line, transmission line and distribution efficiency, step-down transformer efficiency from the transmission line to the distribution network, and the efficiency of distribution network transformers and cables. Nourai *et al.* (2008) reported an overall transmission-and-distribution efficiency of approximately

$$\eta_{\text{TD}} = 0.88,$$

which is adopted here. Incidentally, Papazoglou (1994) provided a formula for finding the minimum possible transmission and distribution losses. He showed, for example, that for a 760 kV, 50 Hz, 1200 km long transmission line having certain other specified properties, the theoretical maximum of the transmission efficiency is 95.21%.

3.4 Overall Efficiency of the Electric Grid

Based on the above values, the average generation-weighted efficiency of the U.S. electric grid is

$$\begin{aligned} \eta_{\text{grid}} &= \eta_{\text{plant}}\, \eta_{\text{TD}} \\ &= (0.347)(0.88) \\ \eta_{\text{grid}} &= 0.31 \end{aligned}$$

3.5 Battery Charging & Electric Vehicle Efficiency

We now arrive at the component in the system whose efficiency is often quoted in connection with electric vehicles—the vehicle itself. Because the efficiency measurements by De Gennaro *et al.* (2014) used below include charging losses, the charging efficiencies reported by Sears *et al.* (2014) (84% during Level 1 charging; 89% during Level 2 charging) are mentioned for comparison and are not applied as an additional efficiency factor.

Conditions	NEDC	WLTC	WMTC
23°C, HVAC Off	78.0%	86.3%	85.7%
23°C, HVAC On	69.4%	79.1%	77.7%
-7°C, HVAC Off	75.3%	77.3%	80.8%
-7°C, HVAC On	42.7%	55.3%	57.4%
Average:	**72%**		

Table 5. Combined charging and vehicle energy conversion efficiency for three different duty cycles (De Gennaro *et al.* 2014).

As shown in Table 5, the unweighted average of the twelve efficiencies was:

$$\eta_{\text{charg}}\,\eta_{\text{car}} = 0.72\,.$$

After reviewing this table, we see where one of the advantages of the gasoline engine is showcased. With the electric vehicle option, waste heat is exhausted in a remote field wherever the power plant happens to be located, whereas with gasoline engines, the waste heat is available to the vehicle owner as an effectively limitless supply of heat during the cold weather months. (In practical operation, the waste heat produced by gasoline engines has proven sufficient for passenger heating throughout more than a century of vehicle operation, without the need for an auxiliary heating system in virtually all operating environments.)

3.6 Overall Efficiency of the Electric Vehicle Option

Factoring in the grid efficiency and the combined charging-and-vehicle efficiency brings the overall efficiency of the electric-vehicle option to:

$$\begin{aligned}\eta_{\text{BEV}} &= \eta_{\text{grid}}\,\eta_{\text{charg}}\,\eta_{\text{car}} \\ &= (0.31)(0.72) \\ &\boxed{\eta_{\text{BEV}} \approx 22\%}\end{aligned} \tag{23}$$

which is less than the efficiency of the Buick gasoline engine, computed in (12) to be $\eta_{\text{g}} = 28\%$. Therefore, even the two-decade-old Buick 3.8-liter 3800 Series III V6 gasoline engine is more energy efficient than the battery-electric vehicle system examined above.

4. Additional U.S. Electrical Generation Required

The preceding analysis also permits an estimate of the additional electrical generation that would be required of the U.S. electric grid if the transportation presently powered by gasoline were instead powered by BEVs. In 2024, approximately 136 billion gallons of gasoline were consumed in the United States (USEIA 2026). Using a gasoline density of 6.2 lb/gal and a lower heating value of 44,000 kJ/kg, the corresponding annual gasoline energy consumption is 1.68×10^{16} kJ/yr or

$$E_g = 4.67 \times 10^{12} \text{ kWh/yr.}$$

Using the gasoline-vehicle efficiency of $\eta_g = 0.28$ calculated above, the mechanical work presently obtained from this gasoline is (assuming the same efficiency of $\eta_g = 0.28$) therefore

$$\begin{aligned} W_g &= \eta_g E_g \\ &= (0.28)(4.67 \times 10^{12}) \\ &= 1.309 \times 10^{12} \text{ kW h/yr} \end{aligned}$$

For a BEV to provide the same mechanical work, electricity leaving the generating plants must subsequently pass through the transmission and distribution system, battery-charging process, and vehicle. From §3.3 through §3.5, the combined efficiency of these processes is

$$\begin{aligned} \eta_{\text{grid-wheel}} &= \eta_{\text{TD}}\, \eta_{\text{charg}}\, \eta_{\text{car}} \\ &= (0.88)(0.72) \\ &= 0.63 \end{aligned}$$

So the additional electrical energy that must be generated to provide the work above is

$$E_{\text{BEV}} = \frac{W_g}{\eta_{\text{grid-wheel}}} = \frac{1.309 \times 10^{12} \text{ kW h/yr}}{0.63} = 2.08 \times 10^{12} \text{ kW h/yr}$$

Meanwhile, U.S. utility-scale net electrical generation in 2024 was 4.309×10^{12} kWh/yr (USEIA 2025c). This means that replacing the present gasoline usage with electricity supplied through the existing generation mix would require annual U.S. electrical generation to increase by approximately 48%:

$$\frac{2.08 \times 10^{12}}{4.309 \times 10^{12}} = 0.48\,.$$

This would, of course, be in addition to the extra charging stations that would be needed.

5. Conclusion

The purpose of this paper is to provide a transparent engineering comparison of the operational energy efficiencies of representative gasoline-powered and battery-electric transportation systems. It has been shown here that gasoline-powered transportation likely has a higher operational energy efficiency than the battery-electric transportation based on the existing U.S. electricity generation. The methodology developed here provides a consistent framework for future comparisons, should the factors involved change.

References

Dababneh, F., Aldababneh, H. Z., & Yang, Y., "Third-party electric vehicle battery remanufacturing supply chains," *Cleaner Logistics and Supply Chain* **15** (2025) 100218.

De Gennaro, M., Paffumi, E., Martini, G., Manfredi, U., Scholz, H., Lacher, H., Kuehnelt, H., & Simic, D., "Experimental Investigation of the Energy Efficiency of an Electric Vehicle in Different Driving Conditions," *SAE Technical Paper 2014-01-1817* (2014).

Dick, A., Greiner, J., Locher, A., & Jauch, F., "Optimization Potential for a State of the Art 8-Speed AT," *SAE International Journal of Passenger Cars—Mechanical Systems* **6** (2013) pp. 899–907.

Evans, A., Strezov, V., & Evans, T. J., "Assessment of sustainability indicators for renewable energy technologies," *Renewable and Sustainable Energy Reviews* **13** (2009) pp. 1082–1088.

Faria, R., Moura, P., Delgado, J., & de Almeida, A. T., "A sustainability assessment of electric vehicles as a personal mobility system," *Energy Conversion and Management* **61** (2012) pp. 19-30.

GE Energy, "7FA Heavy Duty Gas Turbine Product Evolution," *GE 7FA Brochure* (2009) 12 pp.

Liu, Z., Song, J., Kubal, J., Susarla, N., Knehr, K. W., Islam, E., Nelson, P., & Ahmed, S., "Comparing total cost of ownership of battery electric vehicles and internal combustion engine vehicles," *Energy Policy* **158** (2021) 112564.

Loy-Benitez, J., Safder, U., Nguyen, H.-T., Li, Q., Woo, T.-Y., & Yoo, C. K., "Techno-economic assessment and smart management of an integrated fuel cell-based energy system with absorption chiller for power, hydrogen, heating, and cooling in an electrified railway network," *Energy* **233** (2021) 121099.

McKenzie, K. A., "Sun, wind and waves: EV fossil fuel use and emissions on an isolated, oil-dependent Hawaiian island," *World Electric Vehicle Journal* **12** (2021) 87.

National Research Council, *Cost, Effectiveness, and Deployment of Fuel Economy Technologies for Light-Duty Vehicles*, National Academies Press, Washington, DC (2015), Appendix J.

Nourai, A., Kogan, V. I., & Schafer, C. M., "Load Leveling Reduces T&D Line Losses," *IEEE Transactions on Power Delivery* **23** (2008) pp. 2168-2173.

Papazoglou, T. M., "Maximum efficiency of interconnected transmission lines," *IEE Proceedings-Generation Transmission and Distribution* **141** (1994), pp. 353-356.

Pokharel, S., Sah, P., & Ganta, D., "Improved prediction of total energy consumption and feature analysis in electric vehicles using machine learning and Shapley additive explanations method," *World Electric Vehicle Journal* **12** (2021) 94.

Sandoval, E. M., "Eficiencia energética: Motores de combustión interna vs. motores eléctricos" ("Energy efficiency: Internal combustion engines vs. electric motors", *Revista Multidisciplinar de Estudios Generales* **2** (2023) pp. 18–27.

Sears, J., Roberts, D., & Glitman, K., "A comparison of electric vehicle Level 1 and Level 2 charging efficiency," *2014 IEEE Conference on Technologies for Sustainability* (*SusTech*) (2014) pp. 255-258.

Sheng, K., Dibaj, M., & Akrami, M. "Analysing the cost-effectiveness of charging stations for electric vehicles in the U.K.'s rural areas," *World Electric Vehicle Journal* **12** (2021) 232.

Sweeting, W. J., Hutchinson, A. R., & Savage, S. D., "Factors affecting electric vehicle energy consumption," *International Journal of Sustainable Engineering* **4** (2011) pp. 192–201.

U.S. Energy Information Administration, "Table 8.1. Average Operating Heat Rate for Selected Energy Sources, 2014 through 2024," *Electric Power Annual*, U.S. DOE (2025a).

U.S. Energy Information Administration, "Table 8.2. Average Tested Heat Rates by Prime Mover and Energy Source, 2014–2024," *Electric Power Annual*, U.S. Department of Energy (2025b).

U.S. Energy Information Administration, "Table 1.2. Summary Statistics for the United States, 2014–2024," *Electric Power Annual*, U.S. Department of Energy (2025c).

U.S. Energy Information Administration, "Table 1.7.C. Utility Scale Facility Net Generation from Natural Gas by Technology: Total (All Sectors)," *Electric Power Monthly*, U.S. DOE (2025d).

U.S. Energy Information Administration, *State Energy Data System (SEDS): Motor Gasoline Consumption Estimates, 2024*, U.S. Department of Energy (2026).

Waseem, M., Lakshmi, G. S., Ahmad, M., & Suhaib, M., "Energy storage technology and its impact in electric vehicle: Current progress and future outlook," *Next Energy* **6** (2025) 100202.